

[Original Paper]

Improved sensitivity in the quantitative diagnosis of
ischemia based on end-systolic images obtained by
gated SPECT

Yuji Mikami, Yoichi Kuwabara, Toru Kuroda,
Koki Matsuno, Kiyotaka Fujii and Yoshiaki Masuda

(Received December 7, 2000, Accepted December 26, 2000)

SUMMARY

Purpose: To assess the improvement in sensitivity of the quantitative diagnosis of ischemia based on end-systolic images obtained by ECG-gated myocardial SPECT using ^{99m}Tc -tetrofosmin.

Methods: After the intravenous infusion of 740 MBq of ^{99m}Tc -tetrofosmin during stress, we obtained ECG-gated myocardial SPECT images in 17 patients with normal coronary arteries and 81 patients with $\geq 75\%$ coronary artery stenosis. After reconstructing end-systolic, end-diastolic, and summed ungated images, the short axis images were converted to polar maps, and quantitative defect scores were determined based on the extent and severity scores.

Results: In patients with coronary artery disease, their defect scores were significantly greater in end-systolic images than those in end-diastolic and ungated images. In contrast, no differences were observed in the defect scores in patients with normal coronary arteries. After determining the normal limit of the defect scores by using the patients with normal coronary arteries, the sensitivity for detecting ischemia was calculated for end-systolic, end-diastolic and ungated images. The sensitivity was also significantly higher for the end-systolic images than that in end-diastolic or ungated images.

Conclusions: The quantitative diagnosis of ischemia using end-systolic images obtained using ECG-gated myocardial SPECT and ^{99m}Tc -tetrofosmin is more sensitive than other methods without a loss of specificity. Therefore the accuracy of the diagnosis of myocardial ischemia is improved by using end-systolic images.

Key words: coronary artery disease, ^{99m}Tc -tetrofosmin gated SPECT,
quantitative analysis

I. Introduction

Assessment of stress myocardial scintigraphy is usually based on a qualitative visual scoring system, consequently, the assessment may vary greatly between investigators. Therefore, objective evaluation methods of myocardial perfusion using automated, quantitative scoring systems of perfusion defects by comparing with normal values have been developed for most single photon emission computed tomography analysis system. However, the ability to detect ischemia may not be sensitive enough if the normal values vary widely.

With the development of electrocardiogram (ECG) gated ^{99m}Tc myocardial imaging, blood flow and wall motion can be evaluated simultaneously. Because ischemic myocardial segments can be characterized by decreases in both perfusion and systolic function and wall thickening increases radioactivity by partial volume effect[1], SPECT image at end-systole conceptually represent the combined effect of myocardial perfusion and systolic function. The objective of this study was to determine whether the accuracy of quantitative diagnosis of ischemia is improved by systolic image in ECG-gated myocardial stress SPECT images.

II. Materials and Methods

Patients

Seventeen patients with normal coronary arteries (10 men and 7 women; mean age: 64 ± 9 years) and 81 patients with $\geq 75\%$ coronary artery stenosis (58 men and 23 women; mean age: 62 ± 10 years) underwent ECG-gated stress myocardial SPECT. Of the patients with coronary artery disease, there were 53 patients with a lesion in one vessel, 17 patients with lesions in two vessels, and

11 patients with lesions in three vessels. The left coronary artery was involved in 53 patients, the left circumflex artery in 34 patients, and the right coronary artery in 34 patients.

Patients with conduction disturbances such as right or left bundle branch block, or those with arrhythmia such as atrial fibrillation or multiple extra-systole, were excluded from the study.

Myocardial Gated SPECT

Myocardial gated SPECT was performed 40 minutes after the injection of 740 MBq of ^{99m}Tc -tetrofosmin during exercise stress. Data acquisitions were performed using a three-headed gamma camera (Prism 3000XP, Picker Inc.) equipped with low energy, high-resolution parallel hole collimators. Using a $120^\circ \times 3$ imaging arc, SPECT images were acquired in a 64×64 matrix for 72 steps with 70 cardiac cycles per step. The total imaging time was approximately 30 minutes. Images were gated at 16 frames per cycle using a R-wave trigger. The first frame was set for end-diastole and the seventh frame for end-systole. Conventional (ungated) perfusion SPECT images were obtained by summing the gated data into one composite image. Gated SPECT images for end-diastole, and end-systole and the ungated SPECT images were reconstructed into transverse and short-axis images after prefiltering using a Butterworth filter (degree: 7.8; cut-off frequency: 0.20 cycle/pixel.). Polar map displays were then constructed for the short-axis images.

Quantification of perfusion defects

Myocardial perfusion defects were evaluated quantitatively based on extent and severity scores. Calculation of those scores were previously described[2-4]. In brief, a normal range for each pixel has been generated based on the data of the previously selected normal

subject. The extent score was defined as the percent area with a count rate below the normal limit (mean-2SD). The severity score was calculated by summing the differences in regional uptake between patient values and normal values. The extent and severity scores were determined for the end-diastolic, end-systolic, and ungated images respectively. These defect scores were also obtained in 17 patients with normal coronary arteries, and ninety-five percent confidence intervals for the extent and severity scores were determined to determine normal limits of these scores. The defect scores greater than the normal upper limits were defined as "abnormal", and the sensitivities for detecting coronary artery disease were generated, and were compared between the end diastolic, end systolic and ungated images.

Statistical analysis

Data are expressed as mean \pm standard deviation (SD). Paired *t*-test with Bonferroni criteria for multiple comparison was used to examine the difference among quantitative defect scores (extent and severity scores). McNemar test was used to examine the difference of the proportion (sensitivity) between those by end-systolic, end-diastolic and ungated images. *P*-value < 0.05 was considered as statistically significant.

III. Results

Comparison of extent and severity scores in patients with normal coronary arteries (Fig. 1).

There were no differences in the extent or severity scores between end-diastolic or ungated images. The extent score was $7.3 \pm 4.7\%$ for the end-diastolic image, $5.0 \pm 6.8\%$ for the ungated image, and $6.2 \pm 6.1\%$ for the end-systolic image. (*P* = n.s) The severity

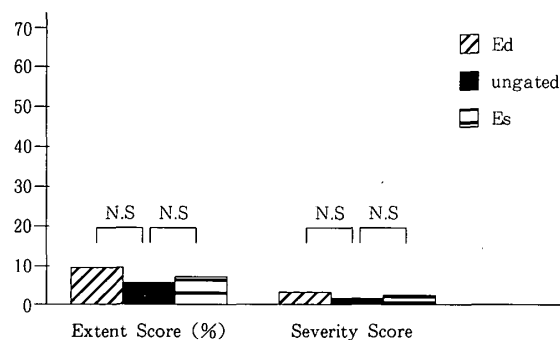


Fig. 1 Comparison of extent and severity scores in patients with normal coronary arteries.

Es : end systolic ; Ed : end diastolic

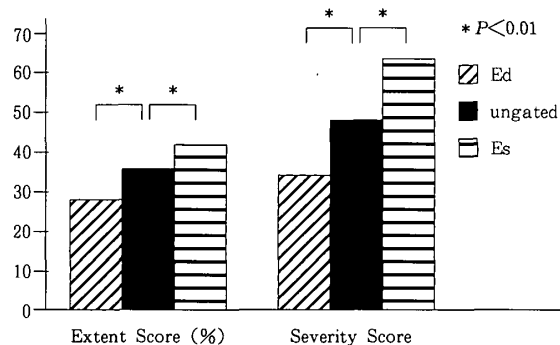


Fig. 2 Comparison of extent and severity scores in patients with coronary artery stenosis.

score was 3.0 ± 2.2 for the end-diastolic image, 1.4 ± 2.4 for the ungated image, and 2.4 ± 3.0 for the end-systolic image. (*P* = n.s)

Comparison of extent and severity scores in patients with coronary artery stenosis (Fig. 2).

There were significant differences in the extent and severity scores between the three types of images in patients with significant stenosis. The extent score was $27.5 \pm 19.6\%$ for the end-diastolic image, $34.4 \pm 21.1\%$ for the ungated image, and $41.8 \pm 19.8\%$ for the end-systolic image. The severity score was 32.8 ± 34.7 for the end-diastolic image, 48.6 ± 51.8 for the ungated image, and 63.6 ± 55.8 for the end-systolic image. Significant statistical difference was observed between any of

two images ($P<0.01$) for both the extent and severity scores.

Comparison between patients with and without myocardial infarction. There were also significant differences in the extent and severity scores between the three types of images, after stratifying patients by means of the history of myocardial infarction. In patient without myocardial infarction ($n=48$), the extent score was $21.5 \pm 15.4\%$ for the end-diastolic image, $28.0 \pm 19.8\%$ for the ungated image, and $41.8 \pm 21.3\%$ for the end-systolic image. Significant statistical difference was observed between the ungated image and end-systolic image, and between the end-diastolic image and end-systolic image ($P<0.01$, Fig. 3). The severity score was 21.7 ± 28.5 for the end-diastolic image, 29.8 ± 28.6 for the ungated image, and 43.6 ± 41.2 for the end-systolic image. ($P<0.01$ for between any two groups)

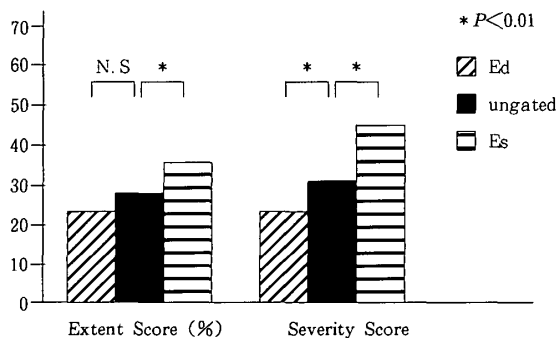


Fig. 3 Comparison between patients with and without myocardial infarction.

Comparison of sensitivities for detecting myocardial ischemia using the quantitative defect score (Fig. 4).

Categorical analysis was performed using sensitivity after defining the normal limits for the extent and severity scores, which were determined by using 95% confidence intervals of these scores in patients with normal coronary arteries. The normal limit

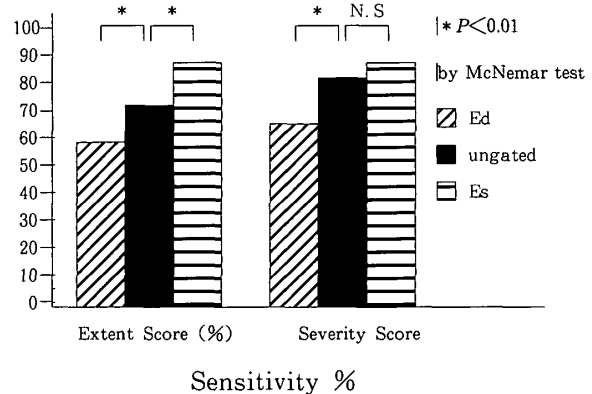


Fig. 4 Comparison of sensitivities for detecting myocardial ischemia using the defect score.

for extent score was 16.6% for the end-diastolic image, 17.0% for the ungated image, and 18.5% for the end-systolic image. The normal limit for the severity score was 7.4 for the end-diastolic image, 6.2 for the ungated image, and 8.4 for the end-systolic image. The sensitivity for detecting coronary artery disease was significantly higher using the end-systolic image than using the ungated or end-diastolic images. Sensitivity was 60.5% for the extent score for the end-diastolic images, 75.3% for the ungated images, and 91.4% for the end-systolic images for the extent scores; ($P<0.01$ between any two images) Sensitivity for the severity score was 67.9% for the end-diastolic images, 85.2% for the ungated images, and 91.4% for the end-systolic images. ($P<0.01$ for end-systolic images versus end-diastolic images, for end-diastolic images versus ungated images. $P=0.06$ for ungated images versus end-systolic images.)

Case presentation

Case 1: Polar map displays for a patient with normal coronary arteries (Fig. 5).

The end-diastolic images are displayed at the top of the figure, and the end-systolic images at the bottom. Both the extent and severity scores were 0 for the end-diastolic

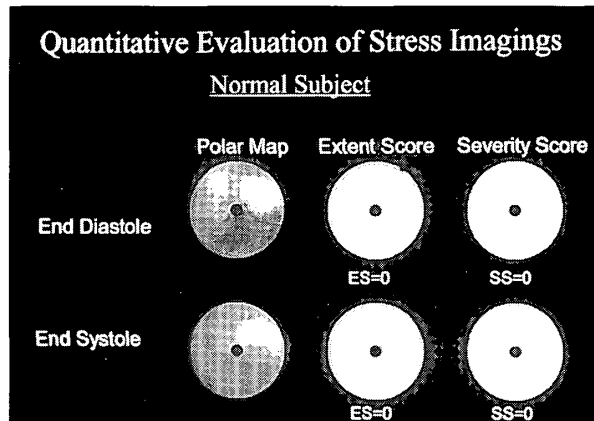


Fig. 5 Polar map displays for a patient with normal coronary arteries.

images as well as the end-systolic images. Hypocount in inferior wall in end-diastolic image is not apparent in end-systolic image.

Case 2: Polar map displays for a patient with a 95% lesion in the left anterior descending artery (Fig. 6).

Both the extent and severity scores were greater for the end-systolic images than for the end-diastolic images. The extent score was 35% for the end-diastolic image and 60 % for the end-systolic image. The severity score was 23 for the end-diastolic image and 76 for the end-systolic image.

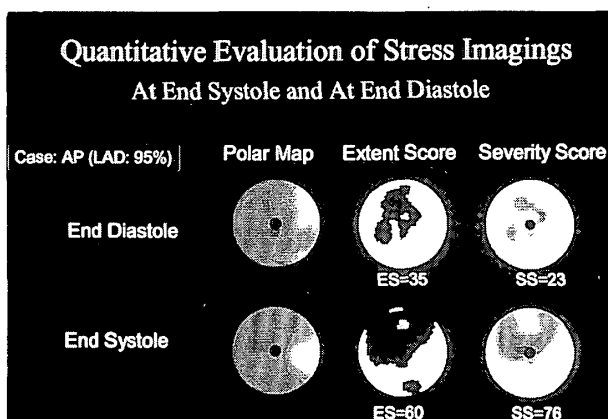


Fig. 6 Polar map displays for a patient with a 95% lesion in the left anterior descending artery.

IV. Discussion

Quantitative determination of perfusion defect scores for SPECT

In order to improve objectivity, several methods of quantitative analysis of SPECT imaging have been introduced. One of the common methods is to construct a polar map, and then normalize the uptake in a given pixel to the maximum uptake, resulting in an uptake ratio (%uptake). This method corresponds to the visual assessment, and the extent of the ischemic region is defined by the area with an uptake ratio lower than an arbitrary cut-off value[5-12]. However, the results of this technique may vary depending on the type of imaging equipment and the imaging agent injected. The presence of attenuation artifact may still lead to an overestimation of the extent of an ischemic region in the inferior wall[13]. More sophisticated quantitative determination of defect scores, extent and severity scores, are calculated by comparing the patient data with normal values obtained in the institute. The extent and severity scores reflected the percentage area of ischemic myocardium and the severity of ischemia, respectively[1-3,14,15]. This method has advantage in adjusting the variation of geographical radionuclide accumulation due to the type of tracer and the gamma camera used. However, these scores may be underestimated if the standard deviations for the normal values become relatively large, which may make it difficult to detect mild myocardial ischemia. Therefore more sensitive resources is desirable to quantitative analysis of perfusion defect.

Wall thickening assessment using ^{99m}Tc myocardial gated SPECT

The short half-life of ^{99m}Tc allows greater amounts of radioactivity to be injected. As

a result, ^{99m}Tc -labeled agents allow us to obtain clear ECG-gated myocardial SPECT images and to evaluate myocardial blood flow and left ventricular wall motion simultaneously [16-20]. This technique also facilitates the diagnosis of myocardial ischemia easy by decreasing an attenuation artifact [21]. In gated SPECT, myocardial images are separately obtained for end-diastole and end-systole. In normal (non-ischemic) region, ventricular wall thicken at systole. Consequently increase in the radioactivity counts between diastole and systole is observed because of the partial volume effect of the accumulated radioisotope [1]. In ischemic region, decreased myocardial blood flow causes a decreased in left ventricular contraction. As a result, the increase in the radioactivity accumulation counts in the ischemic region may be smaller than that in normal regions. Therefore, the difference in the accumulation of ^{99m}Tc -tetrofosmin between ischemic segments and normal segments is expected to be magnified in systolic image [22, 23].

Quantitative determination of perfusion defect by end-systolic image in ECG-gated SPECT

In this study we applied extent and severity scores to ECG-gated myocardial SPECT, and evaluated if identification of ischemic myocardium is more sensitive. So far, no other studies that apply ECG-gating method to quantitative analysis of defect scores on SPECT image have been observed. Both the extent and severity scores were calculated for end-systolic images, end-diastolic images, and summed ungated images. There were no differences in these scores between the end-diastolic, ungated, and end-systolic images in patients with normal coronary arteries. However, in patients with coronary artery

disease, there were significant differences in both extent and severity scores, with end-systolic images showing larger scores than either ungated or end-diastolic images. These results suggest that the quantitative defect scores based on the end-systolic images are more sensitive in detecting myocardial ischemia without increasing the false-positive rate. In fact, sensitivity by using a cutoff value defined by the subjects with normal coronary artery significantly increased in end-systolic image.

The results of this study are quite understandable in patients with obvious myocardial infarction, in which left ventricular contraction is reduced even at rest. Increase in defect scores at systole was also seen in patients without history of myocardial infarction or irreversible defect on rest image. Since abnormal left ventricular systolic dysfunction is basically absent in patient with angina, reason of this result is unclear, but may be partly explained as follows. We acquired the ECG-gated myocardial SPECT images 40 minutes after stress. According to several reports, abnormal wall contraction and relaxation due to the stress-induced myocardial ischemia persist even at this time point [24-29]. This phenomenon may have improved the sensitivity of this study. The presence of hibernating myocardium may also explain the improved sensitivity we found in patients without the evidence of infarction.

V. Limitations of the study

Firstly, ECG-gated myocardial SPECT imaging takes more time than conventional ungated imaging techniques. Furthermore, it takes even longer if the patient has atrial and/or ventricular extrasystoles. It also takes greater amounts of time for the analysis and storage of data because of the large

file size. Secondly, it is difficult to identify systolic SPECT images in patients with irregular R-R intervals, such as in atrial fibrillation. For patients with conduction disturbances such as right or left bundle branch block, asynchronous thickening may be problematic. Thirdly, we used only the end-diastolic and end-systolic images, which mean that 14/16 of the data, were excluded from analysis. Fourthly, the patients in this study include from severe ischemic patients with large myocardial infarction to mild ischemic patients. Therefore, standard deviations of the defect scores are very high. However statistical significance was tested in intra-patient basis, this is not problematic. Finally, we have used a 95% confidence interval based on data from 17 patients with normal coronary arteries to determine the normal range of the extent and severity scores. Therefore, specificity was not obtained in this data set. But the fact that defect scores did not increase at systole in subjects with normal coronary artery suggests that specificity does not decrease in end-systolic images.

VI. Conclusion

In diagnosing cardiac ischemia by myocardial scintigraphy using ^{99m}Tc -tetrofosmin, using gated SPECT to quantitatively assess end-systolic images improves the accuracy of diagnosis, increasing sensitivity without decreasing specificity.

要 旨

^{99m}Tc -Tetrofosmin 心電図同期心筋SPECT像を応用し、その、収縮末期像を用いて虚血診断精度が上がるかどうかを検討した。方法として冠動脈正常例17例及び75%以上の狭窄を持つ冠動脈疾患例81例に負荷時 ^{99m}Tc -Tetrofosmin 740MBq 静注後、心電図同期心筋SPECTを撮像。正常ファイル20例より求めた正常値をもとにし、extent, severity score を収縮末期像 拡張末期像 非同期像それぞれの時相において算出、その値を比較した。ついで正常群の extent, severity score の95%信頼区間を正常上限として冠動脈疾患検出に対する sensitivity も算出、比較検討した。

結果は、冠動脈正常例では extent, severity score とも差を認めなかったのに対し、冠動脈疾患例では extent, severity score とも収縮末期像 非同期像 拡張末期像の順であり、有意差を認めた。冠動脈疾患検出に対する sensitivity も算出し、比較検討したところ extent score では拡張末期像60.5% 非同期像75.3% 収縮末期像91.4%, severity score では拡張末期像67.9% 非同期像85.2% 収縮末期像91.4%と有意に収縮末期像で高かった。

以上より ^{99m}Tc -Tetrofosmin 心電図同期心筋SPECT像を応用し、収縮末期像を用いて定量的診断をすることにより、specificity を下げずに sensitivity が上がり虚血診断精度が向上すると考えられる。

References

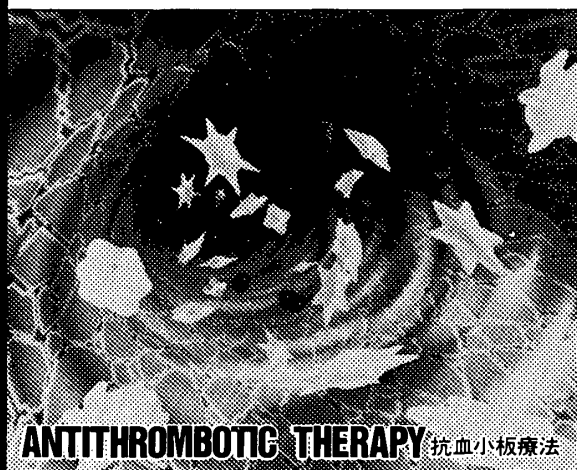
- 1) Calnon DA, Kastner RJ, Smith WH, Segalla D, Beller GA, Watson DD. Validation of a new counts-based gated single photon emission computed tomography method for quantifying left ventricular systolic function: comparison with equilibrium radionuclide angiography. *J Nucl Cardiol* 1997; 4: 464-71.
- 2) Garcia EV, Van Train K, Maddahi J, Prigent F, Friedman J, Areeda J, Waxman A, Berman DS. Quantification of rotational thallium-201 myocardial tomography. *J Nucl Med* 1985; 26: 17-26.
- 3) Klein JL, Garcia EV, DePuey EG, Campbell J, Taylor AT, Pettigrew RI, Amato PD, Folks R, Alazraki N. Reversibility Bull' s-eye: A new polar bull' s-eye map to quantify reversibility of stress-induced SPECT thallium-201 myocardial perfusion defects. *J Nucl Med* 1990; 31: 1240-6.
- 4) Garcia EV, DePuey EG, Sonnemaker RE, Neely HR, DePasquale EE, Robbins WL, Moore WH, Heo J, Iskandrian AS, Campbell J. Quantification of reversibility of stress-induced thallium-201 myocardial perfusion defects: A multicenter trial using bull' s-eye polar maps and standard normal limits. *J Nucl Med* 1990; 31: 1761-5.
- 5) Mahmarian JJ, Pratt CM, Borges-Neto S, Cashion WR, Roberts R, Verani MS. Quantification of infarct size by thallium-201 single-photon emission computed tomography during acute myocardial infarction in man: comparison with enzymatic estimates. *Circulation* 1988; 78: 831-9.
- 6) Mahmarian JJ, Boyce TM, Goldberg RK, Cocanougher MK, Roberts R, Verani MS. Quantitative exercise thallium-201 single-photon emission computed tomography for

- the enhanced diagnosis of ischemic heart disease. *J Am Coll Cardiol* 1990; 15: 318-29.
- 7) Mahmarian JJ, Pratt CM, Cocanougher MK, Verani MS. Altered myocardial perfusion in patients with angina pectoris or silent ischemia during exercise as assessed quantitative thallium-201 single-photon tomography. *Circulation* 1990; 82: 1305-15.
 - 8) Mahmarian JJ, Pratt CM, Boyce TM, Verani MS. The variable extent of jeopardized myocardium in patients with single vessel coronary artery disease: Quantification by thallium-201 single-photon emission computed tomography. *J Am Coll Cardiol* 1991; 17: 355-62.
 - 9) Van Train KF, Areeda J, Garcia EV, Cooke CD, Maddahi J, Kiat H, Germano G, Silagan G, Folks R, Berman DS. Quantitative same-day rest-stress technetium-99m-sestamibi SPECT: definition and validation of stress normal limits and criteria for abnormality. *J Nucl Med* 1993; 34: 1494-502.
 - 10) Van Train KF, Garcia EV, Maddahi J, Areeda J, Cooke CD, Kiat H, Silagan G, Folks R, Friedman J, Matzer L, Germano G, Bateman T, Ziffer J, DePuey EG, Fink-Bennett D, Cloninger K, Berman DS. Multicenter trial validation for quantitative analysis of same-day rest-stress technetium-99m-sestamibi myocardial tomograms. *J Nucl Med* 1994; 35: 609-18.
 - 11) Ceriani L, Verna E, Giovanella L, Bianchi L, Roncari G, Tarolo GL. Assessment of myocardial area at risk by technetium-99m-sestamibi during coronary artery occlusion: comparison between three tomographic methods of quantification. *Eur J Nucl Med* 1996; 23: 31-9.
 - 12) Miller TD, Christian TF, Hopfenspirger MR, Hodge DO, Gersh BJ, Gibbons RJ. Infarct size after acute myocardial infarction measured by quantitative tomographic ^{99m}Tc sestamibi imaging predicts subsequent mortality. *Circulation* 1995; 92: 334-41.
 - 13) Tung C-H, Gullberg GT, Zeng GL, Christian PE, Datz FL, Morgan HT. Non-uniform attenuation correction using simultaneous transmission and emission converging tomography. *IEEE Transactions on nuclear science* 1992; 39: 1134-43.
 - 14) Matzer L, Kiat H, Van Train k, Germano G, Papanicolaou M, Silagan G, Eigler N, Maddahi J, Berman DS. Quantitative severity of stress thallium-201 myocardial perfusion single-photon emission computed tomography defects in one-vessel coronary artery disease. *Am J Cardiol* 1993; 72: 273-9.
 - 15) Kang X, Berman DS, Van Train KF, Amanullah AM, Areeda J, Friedman JD, Kiat H, Germano G. Clinical validation of automatic quantitative defect size in rest technetium-99m-sestamibi myocardial perfusion SPECT. *J Nucl Med* 1997; 38: 1441-6.
 - 16) Takeda T, Toyama H, Ishikawa N, Satoh M, Masuoka T, Ajisawa R, Iida K, Jin W, Sugishita Y, Itai Y. Quantitative phase analysis of myocardial wall thickening by technetium-99m 2-methoxy-isobutyl-isonitrite SPECT. *Ann Nucl Med* 1992; 6: 69-78.
 - 17) Berman DS, Kiat HS, Van Train KF, Germano G, Maddahi J, Friedman JD. Myocardial perfusion imaging with technetium-99m-sestamibi: comparative analysis of available imaging protocols. *J Nucl Med* 1994; 35: 681-8.
 - 18) Cooke CD, Garcia EV, Cullom SJ, Faber TL, Pettigrew RI. Determining the accuracy of calculating systolic wall thickening using a fast Fourier transform approximation: a simulation study based on canine and patient data. *J Nucl Med* 1994; 35: 1185-92.
 - 19) Chua T, Kiat H, Germano G, Maurer G, Van Yrain KF, Friedman J, Berman DS. Gated technetium-99m-sestamibi for simultaneous assessment of stress myocardial perfusion, postexercise regional ventricular function and myocardial viability correlation with echocardiography and rest thallium-201 scintigraphy. *J Am Coll Cardiol* 1994; 23: 1107-14.
 - 20) Masahiko K, Isao M, Masashi N, Ken S, Kazuyoshi T, Shigeru A, Yutaka K, Kikuhiko H, Masao I. Assessment of ischemic heart disease by dipyrindamole stress electrocardiographic gated myocardial single photon emission computed tomography with technetium-99m tetrofosmin. *J Cardiol* 1998; 32: 253-61.
 - 21) Depuey EG, Rozanski A. Using gated technetium-99m-sestamibi SPECT to characterize fixed myocardial defects as infarct or artifact. *J Nucl Med* 1995; 36: 952-5.
 - 22) Galt JR, Garcia EV, Robbins WL. Effect of myocardial wall thickness on SPECT quantification. *IEEE Trans Med Imag* 1990; 9: 144-50.
 - 23) Ziffer JA, Cook CD, Folks RD, La Pidus AS, Alazraki NP, Gercia EV. Quantitative myocardial thickening assessed with sestamibi: clinical evaluation of a count-based method. *J Nucl Med* 1991; 32: 1006.
 - 24) Kloner RA, Allen J, Cox TA, Zheng Y, Ruiz CE. Stunned left ventricular myocardium after treadmill testing in coronary artery disease. *Am J Cardiol* 1991; 68: 329-34.

- 25) Marzullo P, Parodi O, Sambuce G, Marca ssa C, Gimelli A, Bartoli M, Neglia D, L' Abbate A. Does the myocardium become "stunned" after episodes of angina at rest, angina on effort, and coronary angioplasty? Am J Cardiol 1993; 71: 1045-51.
- 26) Johnson LL, Verdesca SA, Aude WY, Xavier RC, Nott LT, Campanella MW, Germano G. Postischemic stunning can affect left ventricular ejection fraction and regional wall motion on post-stress gated sestamibi tomograms. J Am Coll Cardiol 1997; 30: 1641-8.
- 27) Ambrosio G, Betocchi S, Pace L, Losi MA, Perrone-Filardi P, Soricelli A, Piscione F, Taube J, Squame F, Salvatore M, Weiss J L, Chiariello M. Prolonged impairment of regional contractile function after resolution of exercise induced angina: evidence of myocardial stunning in patients with coronary artery disease. Circulation 1996; 94: 2455-63.
- 28) Robertson S, Feigenbaum H, Armstong WF, Dillon JC, O'Donnell J, McHenry PW. Exercise echocardiography: a clinically practical addition in the evaluation of coronary artery disease. J Am Coll Cardiol 1983; 2: 1085-91.
- 29) Katz A, Force T, Folland E, Aebischer N, Sharma S, Parisi A. Echocardiographic assessment of ventricular systolic function. In: Marcus ML and Braunwald E, editors. Marcus Cardiac Imaging: a Companion to Braunwald's Heart Disease. Philadelphia: WB Saunders. 1996: 297-324.

血液と血管に——プレタール

いま、抗血小板剤は、血管拡張作用を併せもった。



使用上の注意 一抜すいー

- 次の患者には投与しないこと
 - (1)出血している患者(血友病、毛細血管脆弱症、上部消化管出血、尿路出血、喀血、硝子体出血等)
 - (2)妊婦又は妊娠している可能性のある婦人
- 次の患者には慎重に投与すること
 - (1)抗凝薬(ワルファリン等)あるいは抗血小板剤(アスピリン、チクロピジン等)を投与中の患者(血液凝固能検査等を十分に行いながら使用する。)
 - (2)月経期間中の患者
 - (3)出血傾向並びにその素因のある患者
 - (4)重篤な肝障害あるいは腎障害のある患者

効果

- 血小板凝集を抑制し、優れた抗血栓効果を示します。
- 下肢血流を増加させ、末梢の血行動態を改善します。
- 慢性動脈閉塞症に基づく潰瘍、疼痛、冷感等の虚血性諸症状を改善します。
- 1日2回投与により、優れた臨床効果が得られます。

効能・効果

慢性動脈閉塞症に基づく潰瘍、疼痛及び冷感等の虚血性諸症状の改善

※用法・用量、その他の使用上の注意等は、製品添付文書をご参照下さい。

抗血小板剤

プレタール錠⁵⁰100

シロスタゾール製剤 Pletaal®

自社開発

薬価基準収載



製造発売元

大塚製薬株式会社
東京都千代田区神田司町2-9

資料請求先

大塚製薬株式会社 学術部
東京都千代田区神田司町2-2
大塚製薬神田第2ビル

(91.3作成)